Supporting Information

A strategy for programming regulation of *in vitro* transcription with application in molecular circuits

Yingxin Hu,[a,b‡] *Chun Xie,*[a‡] *Fei Xu*[a]*, *and Linqiang Pan*[a]*

[a] Key Laboratory of Image Information Processing and Intelligent Control of Education Ministry of China, School of Artificial Intelligence and Automation, Huazhong University of Science and Technology, Wuhan 430074, Hubei, China

[b] College of Information Science and Technology, Shijiazhuang Tiedao University, Shijiazhuang 050043, Hebei, China

‡The authors contribute equally to this work.

Corresponding author Email: lqpan@mail.hust.edu.cn, fxu@mail.hust.edu.cn

Table of Contents

1 Experimental Procedures

1.1 Materials

All oligonucleotides were ordered from Sangon Biotech Co., Ltd. (Shanghai, China). Unmodified oligonucleotides were purchased with PAGE-purification, and modified oligonucleotides with fluorophore and quencher were purified by HPLC. The DNA oligonucleotides were dissolved in water as the stock solution and quantified using Nanodrop 2000, and absorption intensities were recorded at λ = 260 nm. The sequences of all oligonucleotides are listed in Table S1 and S2. T7 RNA polymerase and NTP were purchased from New England Biolabs. All other chemicals were of analytical grade and used without further purification.

1.2 Methods

1.2.1 DNA hybridization reaction

Unless specifically mentioned, the DNA complexes were formed by mixing corresponding single strands with equal concentrations in 1× RNA Pol reaction buffer. The mixture was annealed in a polymerase chain reaction (PCR) thermal cycler at the reaction condition of 85°C for 5 min, 65°C for 30 min, 50°C for 30min, 37°C for 30min, 25°C for 30min, and finally kept at 25°C.

1.2.2 RNA polymerase transcription reaction

Different concentrations of DNA template were mixed with T7 RNA Polymerase (2U/uL), NTPs (1.5 mM) in 1×RNA Pol reaction buffer to transcribe RNA at 37°C for 60-120 minutes.

1.2.3 Catalytical hairpin assembly reaction

The hairpins H1 and H2 were separately heated at 95°C for 5 minutes and cooled down to 25°C for 2 hours before use. Then, they were respectively incubated with different concentrations of initiator strands at 37°C for 60 minutes.

1.2.4 Fluorescent experiments

All experiments were performed in 1×RNA Pol reaction buffer using real-time fluorescence PCR (StepOnePlus, Applied Biosystems). In a typical reaction, the total volume of the solution

was 25μL and the final concentration of F/Q was 400nM for detection. The FAM fluorescence was monitored at 2 minutes intervals. Fluorescence data were processed by subtracting the initial fluorescence reading which was taken as background. The fluorescence curves were obtained by the average values from at least three times repeat experimental results. All the experiments were conducted at 37°C.

1.2.5 PAGE experiment

The samples were mixed with 6× loading buffer (Takara) or 36% glycerin solution and subjected to electrophoresis analysis on a 12% native polyacrylamide gel. The final concentration of F/Q was 800nM where the it was used in the experiment. The analysis was carried out in 1×TAE buffer (40 mM Tris, 20 mM acetic acid, 2 mM EDTA, pH 8.0) supplemented with 12.5 mM MgCl2 at 90 V for 1-2 hours at 4°C. After Stains-All (Sigma-Aldrich) or EB (ethidium bromide) staining, gels were imaged using the MiniGel (Beijing Sage Creation Science Co, LTD).

1.3 DNA strand sequences

Table S1. Sequences of the Oligonucleotides (5' to 3')

Name	Sequence (5′→3′)	Length （n.t.)
T1	ATTGAAGATGGAATGATAATACGACTCACTATAGG GAGACACTAATGAACTACTACTAC	59
B1(B1-5)	GTAGTAGTAGTTCATTAGTGTCTCCCTATAGTGAGT CG	38
I1(I1-5)	TATTATCATTCCATCTTCAAT	21
B1-4	GTAGTAGTAGTTCATTAGTGTCTCCCTATAGTGAGT CGT	39
I1-4	ATTATCATTCCATCTTCAAT	20
B1-3	GTAGTAGTAGTTCATTAGTGTCTCCCTATAGTGAGT CGTA	40
I1-3	TTATCATTCCATCTTCAAT	19
B1-2	GTAGTAGTAGTTCATTAGTGTCTCCCTATAGTGAGT CGTAT	41
I1-2	TATCATTCCATCTTCAAT	18
A	TATTATCATTCCATCTTCAATCTTCGCCT	29
A*	AGGCGAAGATTGAAGATGGAATGATAATA	29
T2	CAGGCTGCTGATTCGTAATACGACTCACTATAGGG AGACACTAATGAACTACTACTAC	58
I2	GTATTACGAATCAGCAGCCTG	21

I3-0	CAGGCTGCTGATTCGTCATTCCATCTTCAAT	31
I4-0	TATTACGAATCAGCAGCCTG	20
I3-1	CAGGCTGCTGATTCGCATTCCATCTTCAAT	30
I4-1	TATTATCGAATCAGCAGCCTG	21
I3-2	AACTAACATATAATCGATTCCATCTTCAAT	30
I4-2	TATTATCCGATTATATGTTAGTT	23
I3-3	AACTAACATATAATCGTTCCATCTTCAAT	39
I4-3	TATTATCACGATTATATGTTAGTT	24
I3-4	AACTAACATATAATCGTCCATCTTCAAT	28
I4-4	TATTATCATCGATTATATGTTAGTT	25
I31(I41)	CGCGACAGTATCTCGATTCCATCTTCAAT	29
I32	CGTTAGGAGCCGTCGCGAGATACTGTCGCG	30
I33(I44)	TATTATCCGACGGCTCCTAACG	22
I42	CGATGCGACAGGGCACGAGATACTGTCGCG	30
I43	CGTTAGGAGCCGTCGTGCCCTGTCGCATCG	30
TCH	ATGAAGATGAAGCTGATAATACGACTCACTATAGG GAGACACTAATGAACTACTACTAC	59
H1	TATTATCAGTCTCTATCATTATCTTGCTTCATCTTCA TCAAGATAATGATAGAGAC	56
H2	ATTATCTTGATGAAGATGAAGCAAGATAATGATAG AGACGCTTCATCTTCATC	53
I	AAGATAATGATAGAGACTGATAATA	25
T3	CAGGCTGCTGATTCGTAATACGACTCACTATAGGG TATCATTCCATCTTCAATCCGTCGACACACCTGAC AAAGT	75
B3	ACTTTGTCAGGTGTGTCGACGGATTGAAGATGGA ATGATACCCTATAGTGAGTC	54
I5	GTATTACGAATCAGCAGCCTG	21
G1	ACTTTGTCAGGTGTGTCGACGGATTGAAGATGGA ATGATAATA	43
I6	TATTATCATTCCATCTTCAATCCGTCGACACAC	33
F	FAM-GGGAGACACTAATGAACTA	19
Q	GTAGTAGTAGTTCATTAGTGTCTCCC-BHQ1	26

Table S2. Strands used in each circuit

module	Strands
YES	T1, B1(B1-5), B1-4, B1-3, B1-2, I1(I1-5), I1-4, I1-3, I1-2
INHIBIT	T1, B1, A, A*
Parallel circuit	T1, B1, I1, T2, I2
2-input AND	T1, B1, I3-0, I4-0, I3-1, I4-1, I3-2, I4-2, I3-3, I4-3, I3-4, I4-4
3-input AND	T1, B1, I31, I32, I33

4-input AND	T1, B1, I41, I42, I43, I44
CHA-based circuit	TCH, B1, H1, H2, I
Cascading circuit	T3, B3, I5, G1, I6, T1, B1
Reporter	F, Q

2 Results and Discussion

2.1 Single-input regulation of the transcription and the YES circuit

We firstly verified the formation of the complete template by three strands T1, B1-i, and I1-i (i=2, 3, 4, and 5). From the gel results (Figure S1b, c), upon addition of the input strand I1-i, a slightly slower band corresponding to the T1/B1-i/I1-i was observed, indicating that the template with nicked promoters was well assembled. Here, the band of strand I1-i (i=5,4,3, and 2) blurred due to its low sensitivity towards EB. The fluorescence experiments in Figure 2 indicated that a robust performance was achieved when i = 5 was chosen as the nick position of the promoter. Thus, a single-input YES transcriptional circuit was established in which T1/B1-5 acted as the incomplete template and I1-5(I1) as the input.

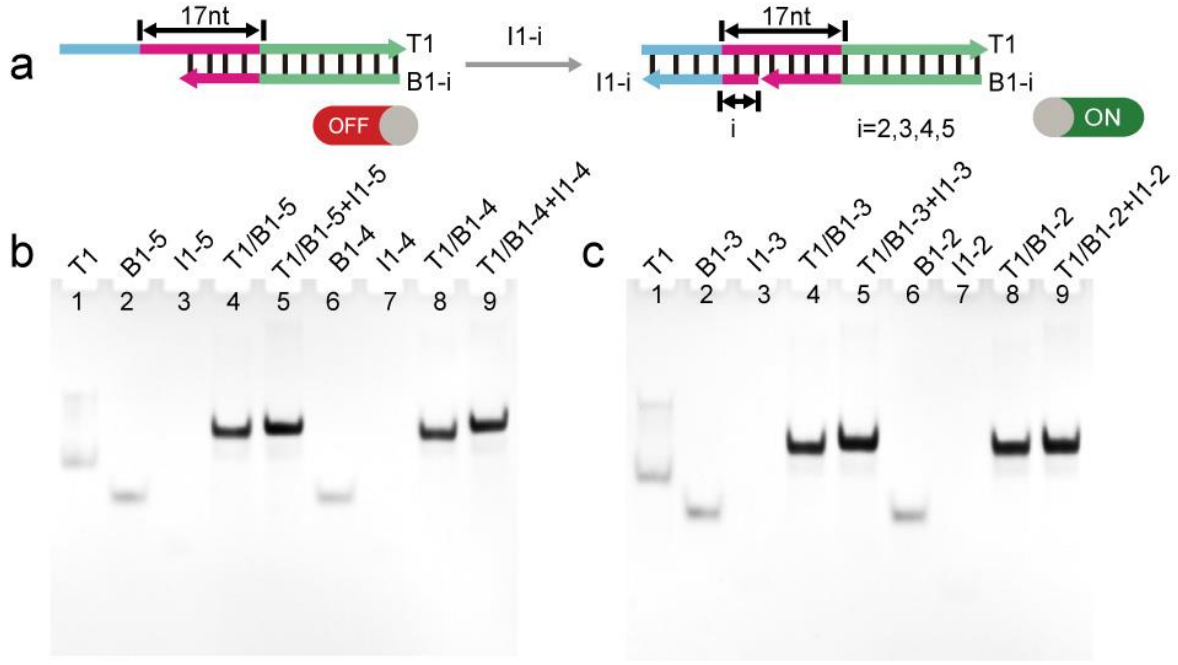

Figure S1. The single-input self-assembled transcriptional template with nicked promoter. (a) Schematic illustration of the state change of the RNA transcription template From OFF state to ON state. (b-c) 12% Native PAGE analysis of the formation of the assembled template where i = 2, 3, 4, and 5, respectively. DNA strands added in every lane are indicated above the image, the assembled structure was represented by its elements seperated by slashes. Concentrations for each sample are all 1μM.

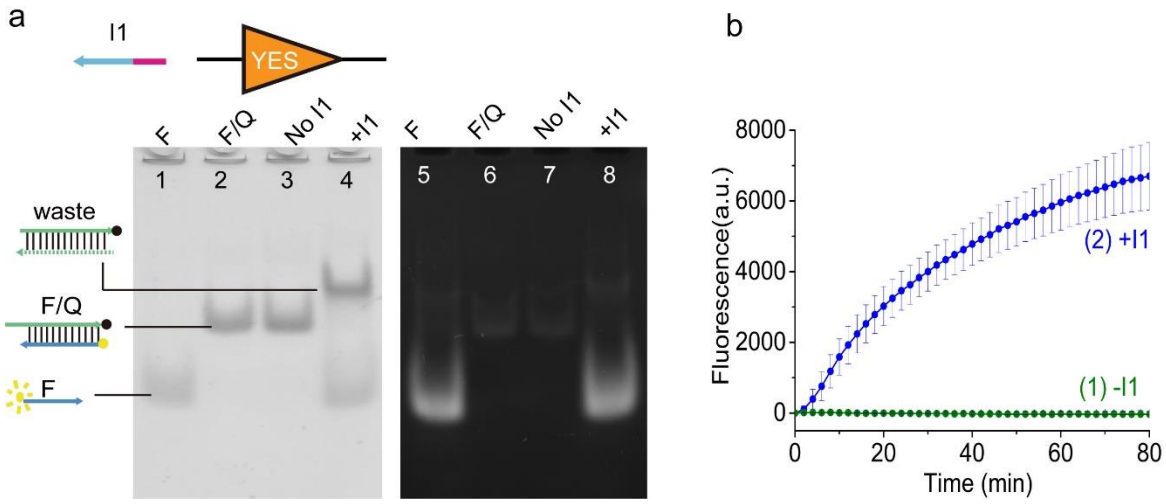

Figure S2. (a) 12% Native PAGE analysis of the YES circuit. The final concentration of DNA templates T1/B1-5 and I1 was 20nM, 20nM respectively. Gel results from lanes 1−4 were detected with Stains-All under white light, while the results from lanes 5−8 were imaged under UV light without staining. (b) Time-dependent fluorescence assay to measure the kinetics of the YES circuit in the absence and presence of I1. Final concentrations of the circuit complex T1/B1-5 and I1 were 10nM respectively.

To confirm the effectiveness of the YES citcuit, the native PAGE gel was performed. As shown in Figure S2a, in the presence of I1(I1-5), the band of F/Q disappeared and a slower-migration band corresponding to the Q/RNA was observed (lane 4). Accordingly, fluorescence strand F appeared in lane 8. In contrast, in the absence of I1 (lane 3), the band of F/Q kept unchanged and no F was observed in lane 7. The gradual increase of the fluorescence signal in the presence of input and the unchanged fluorescence signal without the input also verified the YES operation (Figure S2b).

2.2 2-input INHIBIT circuit

As shown in Figure S3a, the addition of strand A initiated the transcription by switching the the template from OFF state to ON state. Because the hybridization of A with A* has more base pairs than its hybridization with T1/B1-5, strand A was prone to hybridize with A*. Thus, the transcription template was still incomplete. The kinetics analysis of the circuit in Figure S3b verified the designed logic. Upon the addition of strand A, the fluorescence signal has a gradual increase. Whether A was present or not, once ‘A*’ was added to the sample, there was no distinct change of the fluorescence signal.

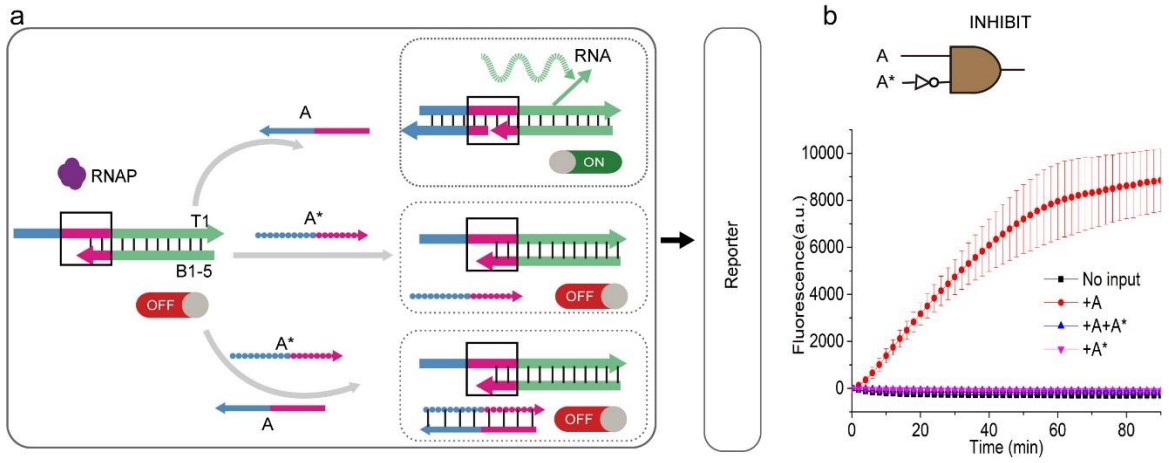

Figure S3. (a) Operating mechanism of the INHIBIT circuit, A* is complementary to A. (b) Time-dependent fluorescence assay to measure the kinetics of the circuit. Final concentrations of the gate complex T1/B1-5, A, and A * were 10nM, 10nM, and 10nM, respectively.

2.3 Multi-input regulation of the transcription and the AND circuit

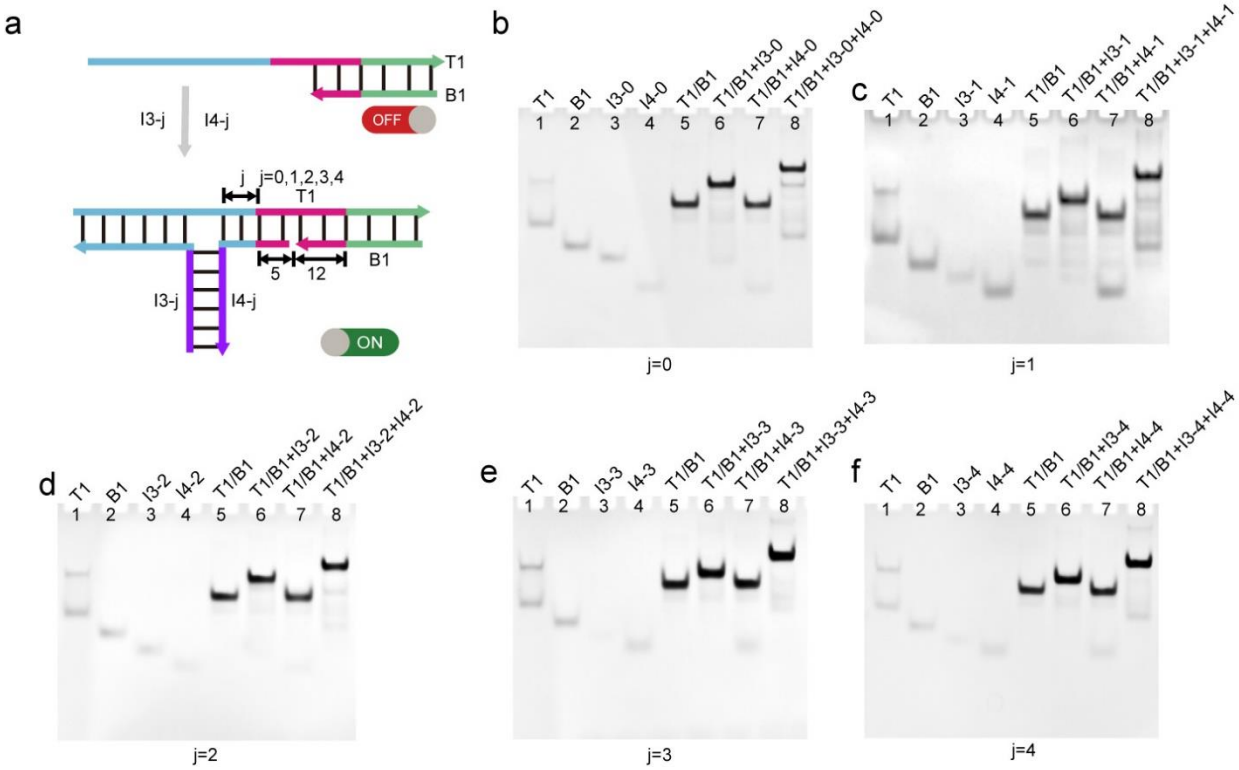

Figure S4. The two-input self-assembled transcriptional template with nicked promoter. (a) Schematic illustration of the state change of the RNA transcription template From OFF state to ON state based on a three-way junction structure. (b-f) 12% PAGE gel analysis of the assembled template with nicked promoters where j=0, 1, 2, 3, and 4, respectively. DNA strands added in every lane are indicated above the image. Concentrations for each sample in the PAGE gel are all 1μM.

To explore the transcription efficiency of the multi-input assembled template based on three-way junction structure, different length (j=0, 1, 2, 3, and 4) was examined (Figure S4a). We first tested the reaction products after the addition of inputs to the gate complex T1/B1 (Figure S4b-f). The presence of I3-j led to the appearance of a new, slow-moving band corresponding to T1/B1/I3-j (lane 6), whereas upon addition of I4-j, the band migrated the same distance with T1/B1 and I4-j was still observed (lane 7), indicating that the strand I4-j alone could not hybridize with T1. It was observed that the band T1/B1 almost disappeared and a band with significantly slower migration corresponding to the T1/B1/I3-j/I4-j appeared (lane 8) in the presence of the two inputs. Although there existed some unexpected structures, the majority of the band was well-formed T1/B1/I3-j /I4- j. The experimental results suggested that only the cooperative interactions of the two inputs could yield a complete template.

The fluorescence experiments in Figure 3 indicated that a robust performance was achieved when j = 2 was chosen as the junction position of the template. Thus, a two-input AND transcriptional circuit was established in which T1/B1-5 acted as the incomplete template and I3-2(I3) and I4-2(I4) as the input.

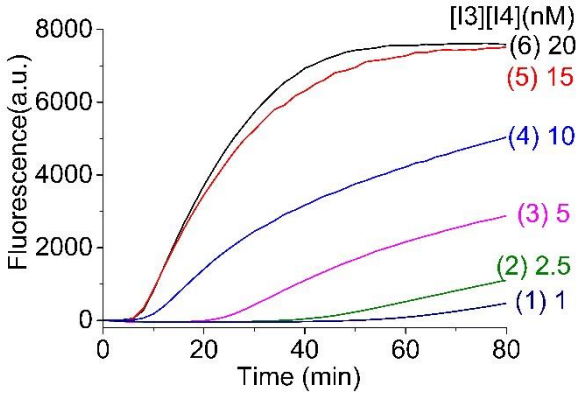

Figure S5. Fluorescence intensity analysis of the 2-input AND circuit with different concentrations of inputs. The final concentrations of DNA templates were 20nM.

To explore the kinetics of the 2-input AND circuit, a series of concentrations of inputs were employed to activate the circuit by fluorescence assay (Figure S5). As expected, with the increase of the inputs, there was an elevation of the fluorescence accordingly. It's noteworthy that the samples with the concentration of 15 and 20nM almost had the same growth trends and they reached the plateau quickly. Different from the linear template in the YES and parallel transcription circuit, the template with a three-way junction in the AND circuit seemed to have a relatively slower reaction rate. The possible reason may be that the synergistic action of the two inputs with the gate complex had a slightly lower yield than the single input hybridization.

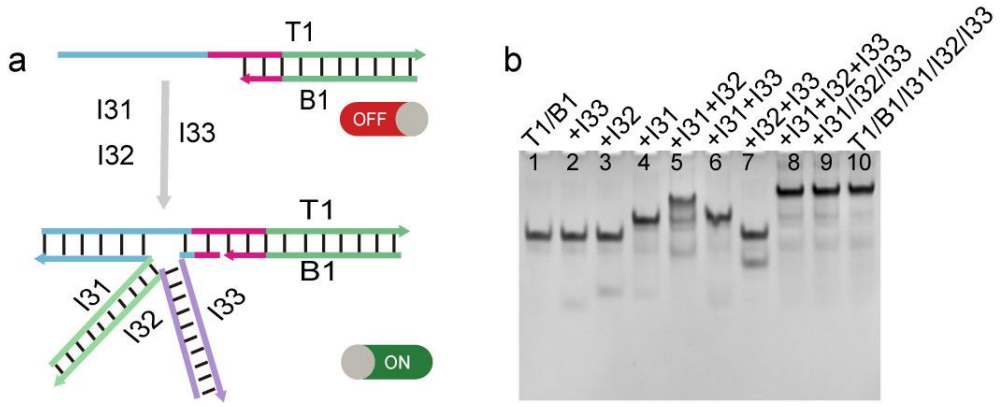

Figure S6. (a) Schematic illustration of the state change of the transcription template from OFF state to ON state by three inputs. (b) Native PAGE gel analysis of the assembled structure upon the addition of different inputs. lane 1: T1/B1; lane 2: T1/B1+I33; lane 3: T1/B1+I32; lane 4: T1/B1+I31; lane 5: T1/B1+I31+I32; lane 6: T1/B1+I31+I33; lane 7: T1/B1+I32+I33; lane 8: T1/B1+I31+I32+I33; lane 9: T1/B1+I31/I32/I33 in which I31/I32/I33 represents the annealed structure; lane 10: the annealed structure T1/B1/I31/I32/I33. Concentrations for each sample in the PAGE assay are all 1μM.

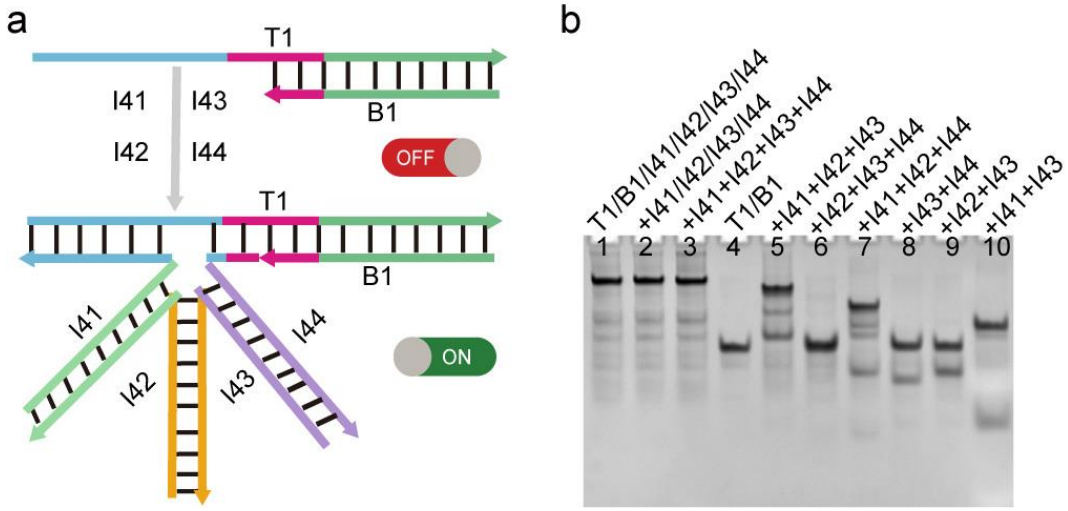

Figure S7. (a) Schematic illustration of the state change of the self-assembled transcription template from OFF state to ON state by four inputs. (b) Native PAGE gel analysis of the assembled structure upon the addition of different inputs. lane 1: the annealed structure T1/B1/I41/I42/I43/I44; lane 2: T1/B1+I41/I42/I43/I44, I41/I42/I43/I44 represents the annealed structure; lane 3: T1/B1+I41+I42+I43+I44; lane 4: T1/B1; lane 5: T1/B1+I41+I42+I43; lane 6: T1/B1+I42+I43+I44; lane 7: T1/B1+I41+I42+I44; lane 8: T1/B1+I43+I44; lane 9: T1/B1 +I42+I43; lane 10: T1/B1 +I41+I43. Concentrations for each sample in the assay are all 1μM.

After confirmation of the 2-input regulation of the transcription, other multi-input such as 3-input and 4-input AND circuits were also investigated. The design of 3-input and 4-input gates was similar to the dual-input. Similar to the previous circuit, the formation of the complete template assembled from the gate complex T1/B1 and multiple inputs was firstly verified PAGE

gel analysis. As shown in Figure S6 and S7, without the assistance of I31(I41), I33 (I44) could not hybridize with the gate complex. Only under the cooperative action of all the input strands, the complete template could form, indicated by a new band with the same mobility identical to annealed T1/B1/I31/I32/I33 (T1/B1/I41/I42/I43/I44).

The fluorescence results of the regulation with different number of inputs (YES circuit, 2-input AND circuit, 3-input AND circuit, and 4-input AND circuit) was investigated. As shown in Figure S8a, the assembled template with only a single input (YES circuit) had the fastest kinetics, and the template with a gap formed by two (2-input AND circuit) or three inputs (3-input AND circuit) had a slightly decreasing rate. In contrast, the fluorescence of the template with four inputs (4-input AND circuit) decreased dramatically, which might result from the low yield of the multi-way junction structure without annealing. Figure S8b gave a good explanation, comparing to the direct assembled sample, the pre-annealed sample had a distinct increase in fluorescence. The experiment results indicate that as the number of input increases, the transcription efficiency can be improved by pre-annealing all inputs.

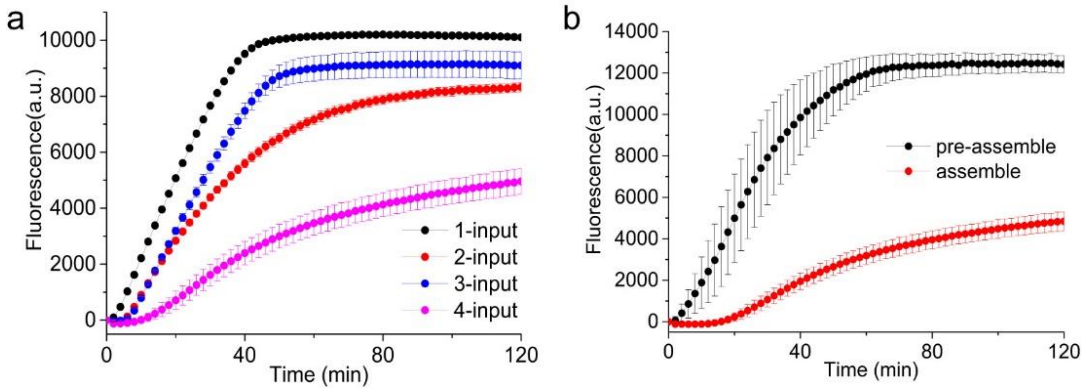

Figure S8. (a) Fluorescence intensity analysis of the transcription circuits with 1, 2, 3, and 4 inputs (corresponding to YES circuit, 2-input AND circuit, 3-input AND circuit, and 4-input AND circuit, respectively). (b) Fluorescence intensity analysis of the 4-input AND circuit with or without annealing process. Final concentrations of DNA templates were 20nM respectively.

2.4 Parallel RNA transcription circuit

We verified the formation of the assembled structures T2/B1/I2 firstly (Figure S9a). Upon addition of I2 to the complex T2/B1, a little slower band in lane 5 was observed and there was no I2 left, demonstrating the well-formed template. To explore the kinetics of the circuit, a series of concentrations of inputs (I1 and I2) were used to switch on the circuit by fluorescence assay (Figure S9b). With the increase of the inputs, the fluorescence signal enhanced accordingly. It's noteworthy that the samples with the concentration of 10, 15, and 20nM almost

had the same growth trends and they reached the plateau quickly. Moreover, the 10nM input of the two-input parellel circuit had a reaction rate similar to that of a 20nM single input because either independent templates could produce the target RNA.

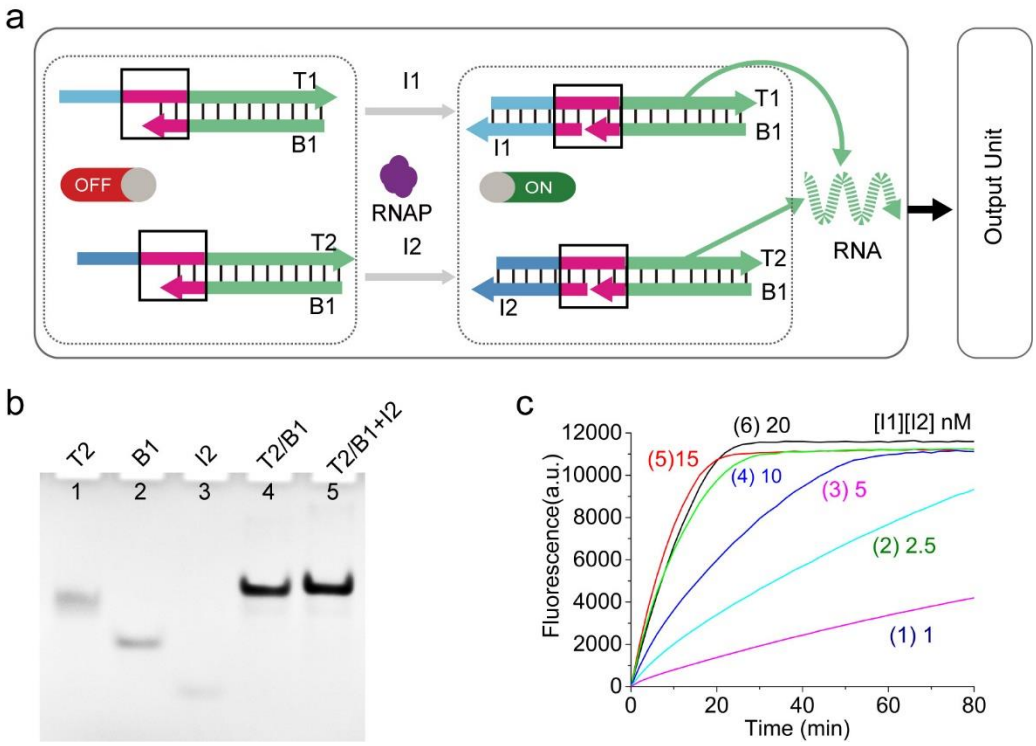

Figure S9. (a) Two-input parallel transcription circuit. (b) 12% Native PAGE analysis of the transcription template T2/B1/I2 with nicked promoters used in the parallel circuit. DNA strands added in every lane are indicated above the image. Concentrations for each sample are all 1μM. (c) Time-dependent fluorescence assay to measure the kinetics of the parallel circuit with different concentrations of inputs. [T1/B1] = 20 nM, [T2/B1] = 20 nM.

2.5 CHA-based regulation of the transcription and the cascading circuit

As shown in Figure S10, the CHA reaction consisted of two hairpin structures H1, H2, and the initiator strand I. In the absence of the strand I, the two hairpins did not interact with each other and kept their hairpin conformation. The addition of I opened H1 through exposed toehold and yielded H1/I. The newly exposed toehold in the assembly H1/I further caused the opening of H2 to produce H1/H2 and released I. The newly generated I initiated a new round of opening of hairpins via toehold-mediated strand displacement, forming double-stranded H1/H2. Gel electrophoresis was carried out to examine the CHA circuit. A negligible new band appeared in lane 5 in the absence of the initiator I, indicating that most of the two hairpin structures did not hybridize unexpectedly. Whereas, as the control sample, a distinct new band was observed in lane 4 when the hairpin structures were annealed. Upon addition of initiator I, a slower band which was the same as the annealed samples corresponding to H1/H2 appeared (lanes 6, 7 and

8). In addition, with the increasing concentration of I, more double-stranded products H1//H2 were generated. The experimental results suggested the successful operation of the CHA circuit.

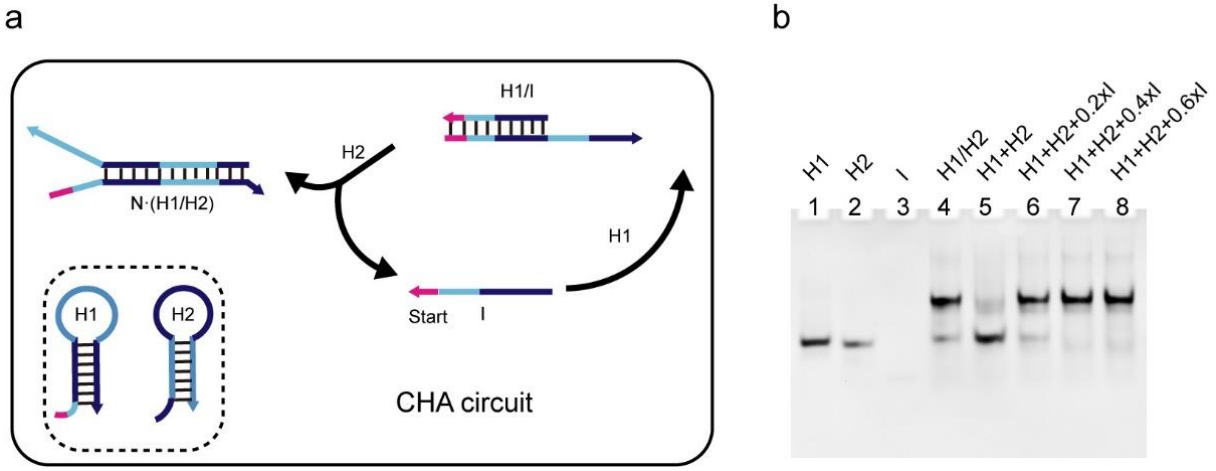

Figure S10. (a) Schematic representation of the CHA circuit. (b) Native PAGE gel analysis of the CHA circuit. DNA strands added in every lane are indicated above the image. Concentrations of the samples for each lane except strand I are all 1μM, the concentration of I was 0.2μM, 0.4μM, and 0.6μM in lane 6, 7, and 8, respectively.

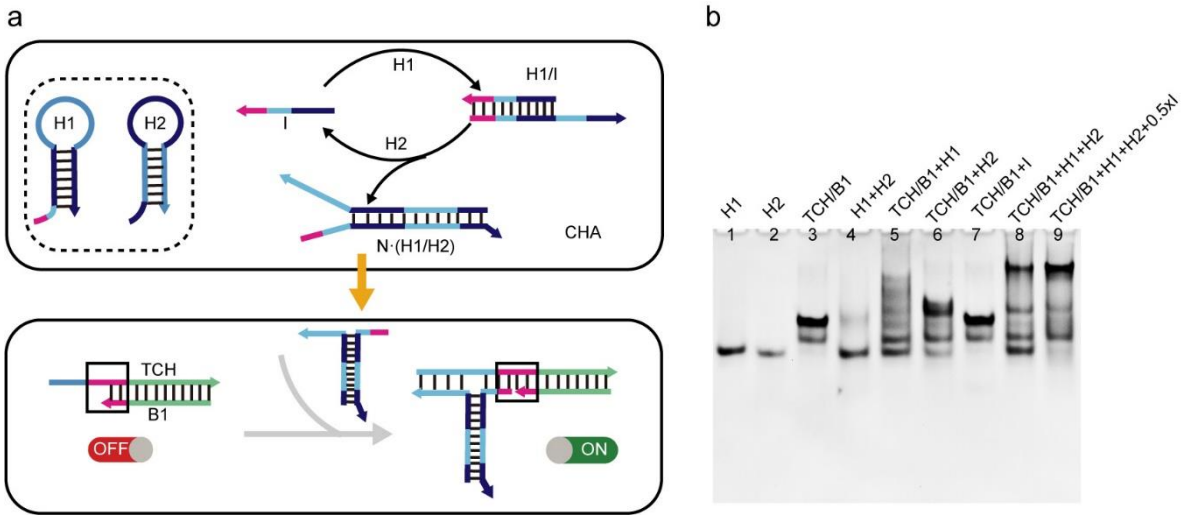

Figure S11. (a) Schematic representation of the transcription template based on CHA reaction. (b) Gel analysis of the assembled structure. DNA strands added in every lane are indicated above the image. [I]=0.5μM, other concentrations for each sample in PAGE are all 1μM.

The CHA-based transcription circuit involves two reactions: upstream CHA and downstream transcription circuit. The downstream transcription is activated upon a successful operation of the CHA circuit. The CHA-based assembly of the template was verified by the gel electrophoresis (Figure S11). a large amount of H1 or H2 remained upon the addition of H1, H2, or H1+H2 into incomplete template TCH/B1 in lane 5, 6, 8 separately. Meanwhile, no new band appeared when strand I was added alone in lane 7. In contrast, in the presence of strand I,

most H1 and H2 were consumed and reacted with TCH/B1 to form a complete transcription template. Overall, the experimental results suggested that the output of the upstream CHA circuit could be integrated with the downstream circuit.

2.6 Transcription circuit-based regulation of and the cascading circuit

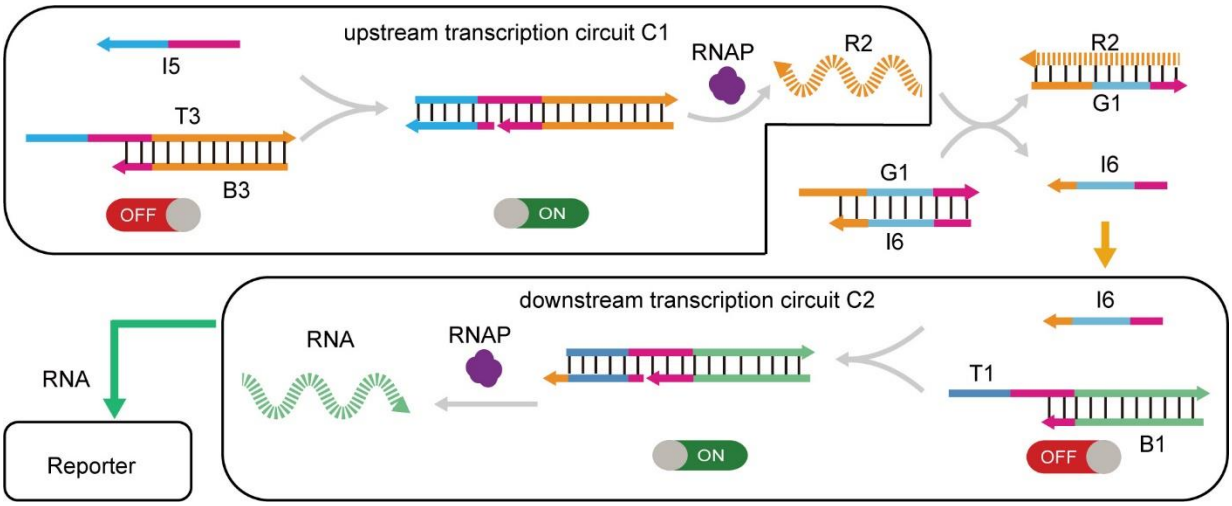

Figure S12. Schematic illustration of the cascaded circuit in which RNA generated from upstream transcription circuit controlled the downstream transcription circuit.

We further tested a two-level concatenated transcription circuit to demonstrate the extensibility of the strategy. As shown in Figure S12, the cascading circuit consisted of an upstream transcription circuit C1 and a downstream transcription circuit C2. Initially, the synthetic template in the circuit C1 was in an OFF-state, and circuit C2 was blocked as the downstream input I6 was insulated in the complex G1/I6. The introduction of strand I5 flipped OFF-template in the circuit C1 to the ON state and RNA strand R2 was transcribed. Subsequently, RNA generated by C1 released I6 from G1/I6 via displacement reaction. Strand I6 was then transmitted to the circuit C2, changing the OFF-state template to ON state. The RNA produced by circuit C2 was measured via the Reporter module. Here, the complex G1/I6 bridged the upstream and downstream circuit and the state of the downstream transcription circuit was dynamically adjusted in response to the upstream circuit.

Before testing the whole circuit, we first verified new elements by native PAGE assay. The disappearance of I5 after its addition to the gate complex T3/B3 suggested that they have self-assembled into the complete template (Figure S13 lane 5).

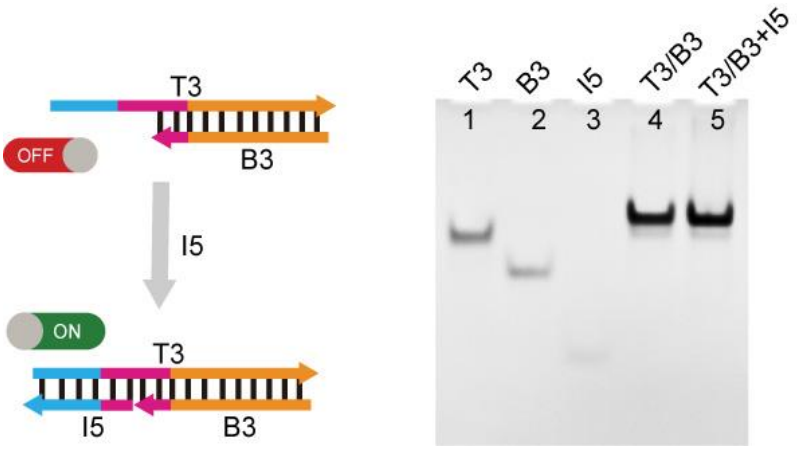

Figure S13. 12% PAGE gel analysis of the template with nicked promoters used in the upstream transcription of the cascading circuit. DNA strands added in every lane are indicated above the image. Concentrations for each sample in the PAGE assay are all 1μM.

Considering that I6 might dissociate from G1/I6 and caused an unwanted leak, we tested the ratio of G1/I6 in the cascading circuit. As shown in Figure S14, upon addition of initiator strand I5, whether the ratio of G1/I6 was 1:1 or 2:1, the fluorescence intensity had a dramatic change. In the absence of strand I5, there was also an enhancement in fluorescence for the sample with the 1:1 G1/I6, this indicated that a leak had occurred. By contrast, only a slightly weak increase in fluorescence was observed when the ratio was 2:1, suggesting that the leak could be suppressed by increasing the ratio of G1 in the complex G1/I6. Based on the results, 2:1 was selected as the ratio of G1 and I6 in the cascading circuit.

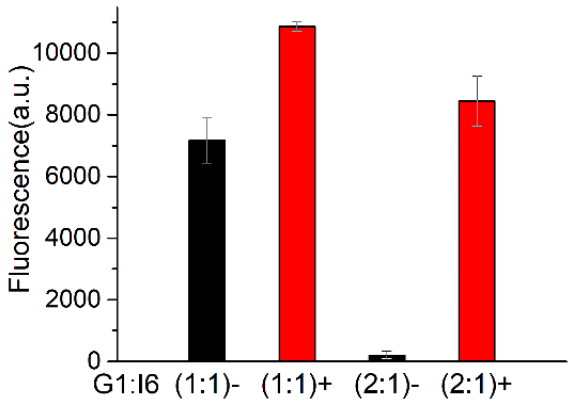

Figure S14. Fluorescence intensity analysis of the effect with different ratios of G1 and I6 in the complex G1/I6 for cascading circuit. (1:1)- or (2:1)- represents the sample without initiator strand and (1:1)+ or (2:1)+ represents the sample in the presence of initiator strand. [T3/B3] =50nM, [I5] =50nM, [G1/I6] =100nM, G1:I6=1:1 or G1:I6=2:1, [T1/B1] =100nM.

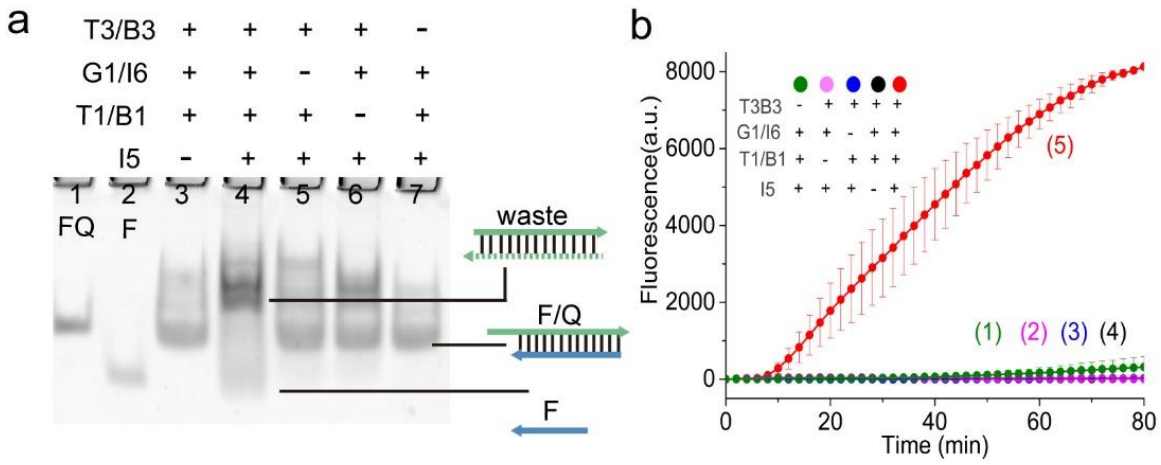

Figure S15. (a) Native PAGE (12%) analysis of the cascading circuit. Lane 1: F/Q, lane 2: F, Lane 3: the circuit in the absence of I5, lane 4: the circuit with I5, lane 5: the circuit in the absence of G1/I6, lane 6: the circuit in the absence of T1/B1, lane 7: the circuit in the absence of T3/B3. (b) Kinetics of the cascading circuit, [T3/B3] =50nM, [I5] =50nM, [G/I6] =100nM, G: I6=2:1, [T1/B1] =100nM.

Then, the functioning of concatenated circuits was verified with a native PAGE gel experiment and a fluorescence assay (Figure 15a and 15b). No new band or obvious change in the fluorescence emerged in the absence of upstream input I5 (lane 3, curve 4), illustrating that the downstream transcription reaction did not occur. When I5 was introduced, F/Q was totally consumed and two strong bands representing Q/RNA and F appeared (lane 4), accompanied by the rise of fluorescence intensity (curve 5), indicating the activation of the downstream transcription. In three control samples without either medium G1/I6 (lane 5, curve 3), downstream template T1/B1 (lane 6, curve 2), and upstream incomplete template T3/B3 (lane 7, curve 1), the F/Q band remained unchanged and no F band appeared, meanwhile the fluorescence intensity remained low. These results suggested that the downstream circuit was indeed activated by the upstream circuit.

Compared with the previous single-layer transcription circuit, fluorescence growth of the cascading circuit had a lag time,which resulted from the upstream transcription reaction and the medium displacement reaction. This indicated that the timing of the downstream signal could be coordinated by changing the concentration of G1 in the complex G1/I6. As displayed in Figure S16, the increase of fluorescence signal with a 4:1 G1/I6 was later than that of 2:1, proving that the time delay could be extended by increasing the concentration of G1.

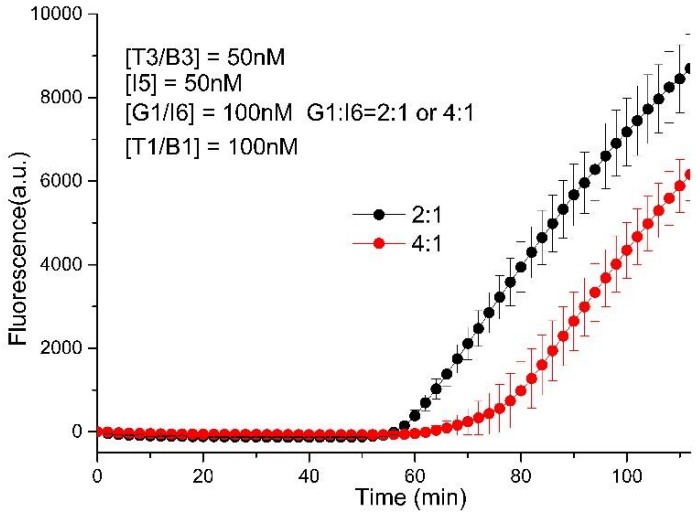

Figure S16. Fluorescence intensity analysis of the time delay by increasing G1 concentration in the complex G1/I6.

Meanwhile, the yield of downstream RNA could also be regulated by changing the concentration of G1/I6 in the cascade circuit because the higher concentration of G1/I6, the more I6 fed into the downstream circuit, which would induce more RNA transcription and a higher fluorescence signal. As shown in Figure S17, the fluorescence growth of G1/I6 at 40nM was significantly faster than that of 20nM, which also confirmed that the production of downstream RNA can be adjusted by changing the G1/I6 concentration.

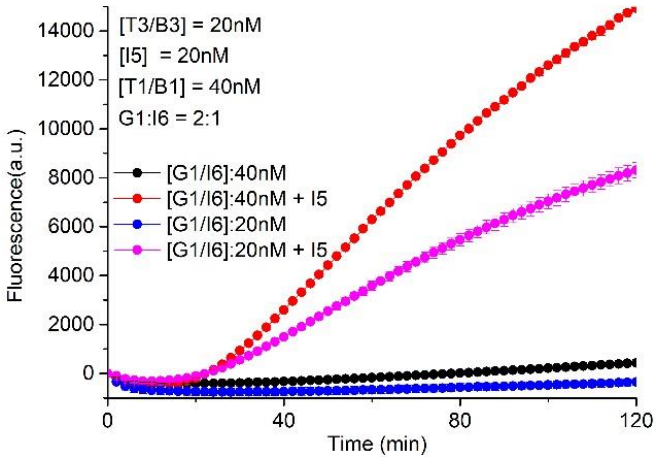

Figure S17. Fluorescence intensity analysis of effect with different G1/I6 concentrations in the cascading circuit. [G1/I6]:40nM(20nM) represents the sample without I5 and [G1/I6]:40nM(20nM) + I5 represents the sample with I5.

2.7 Simulation models of the 2-AND circuit

As shown in Figure S18, the dual-input transcription circuit was triggered by I3 and I4, where incomplete template T/B self-assembled with the inputs to form T/B/I3/I4, which acted

as the substrate for T7 RNA polymerase. After that, T7 polymerase catalyzed the transcription reaction and produce RNA, which then displaced the reporter F/Q and led to a significant fluorescent signal. As depicted above, the reaction can be modeled as following:

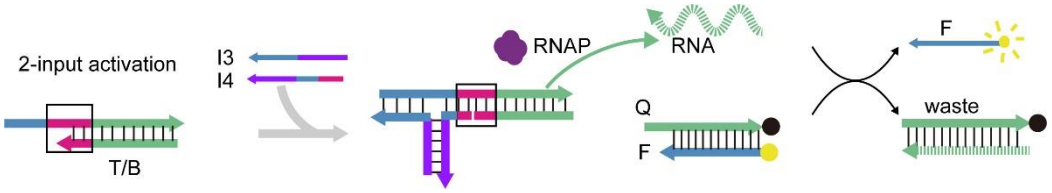

Figure S18. The dual-input transcription circuit

$$\mathrm{T/B + I3 + I4 \xrightarrow{K_1} T/B/I3/I4} \qquad (1)$$

$$\mathrm{T/B/I3/I4 + T7 \xrightarrow{K_p} T/B/I3/I4 + T7 + RNA} \qquad (2)$$

$$\mathrm{RNA + F/Q \xrightarrow{K_2} F + waste} \qquad (3)$$

Equation (1) is a simplified hybridization reaction with the kinetic rate K_1. Equation (2) is a simplified polymerase catalysis reaction with the kinetic rate K_p. Equation (3) is the strand displacement reactions and 'F', waste represent FAM-modified strand and DNA/RNA waste respectively. K_1, K_p, and K_2 are the reaction constants for equations (1) to (3), respectively.

Therefore, the rate equation of T/B/I3/I4 can be derived from equation (1) as:

$$\mathrm{d[T/B/I3/I4]/dt} = K_1\mathrm{[T/B][I3][I4]}$$

The rate equation of RNA can be derived from equation (2) and (3) as:

$$\mathrm{d[RNA]/dt} = K_p\mathrm{[T/B/I3/I4][T7]} - K_2\mathrm{[RNA][F/Q]}$$

The rate equation of F can be derived from equation (3) as:

$$\mathrm{d[F]/dt} = K_2\mathrm{[RNA][F/Q]}$$

Supposed that the initial condition is $[T/B]_0$, $[I3]_0$, $[I4]_0$, $[T7]_0$, $[F/Q]_0$, the mass balance equations are:

$$\mathrm{[T/B]_0 = [T/B] + [T/B/I3/I4]}$$

$$\mathrm{[I3]_0 = [I3] - [T/B/I3/I4]}$$

$$\mathrm{[F/Q]_0 = [F/Q] + [F]}$$

In the simulation, we use the fluorescence signal to directly determine the concentration of F. The differential equations can be obtained as:

$$\mathrm{T/B(k+1) = T/B(k)} - K_1\mathrm{T/B(k)I3(k)I4(k)}$$

$$\mathrm{I3(k+1)} = \mathrm{I3(k)} - K_1\mathrm{T/B(k)I3(k)I4(k)}$$

$$\mathrm{T/B/I3/I4(k+1)} = \mathrm{T/B/I3/I4(k)} + K_1\mathrm{T/B(k)I3(k)I4(k)}$$

$$\mathrm{RNA(k+1)} = \mathrm{RNA(k)} + K_p\mathrm{T/B/I3/I4(k)T7(k)} - K_2\mathrm{RNA(k)F/Q(k)}$$

$$\mathrm{F/Q(k+1)} = \mathrm{F/Q(k)} - K_2\mathrm{RNA(k)F/Q(k)}$$

$$\mathrm{F(k+1)} = \mathrm{F(k)} + K_2\mathrm{RNA(k)F/Q(k)}$$

Suppose that at time *t*, the concentration of reactants in the experiment was *Ce(t)*, and the concentration in the simulated was *Cs(t)*. Taken the Residual Sum of Squares (RSS) as the object function:

$$f = \sum_{t=0}^{t_{max}} (Ce(t) - Cs(t))^2$$

The rate constants were calculated by minimizing the object function. In order to survey the kinetic of the circuit in detail, four control experiments with the varying concentrations of template were performed respectively. After the calculations, the simulation data have a good agreement with the experimental results (Figure S19). Based on the fluorescence results, K_1, K_p, and K_2 for equations (1), (2) and (3) were fit to 4.10×10+15 M-1·s-1, 7.70×10-7 L·unit-1·s-1 and 6.85×10+5 M-1·s-1, respectively.

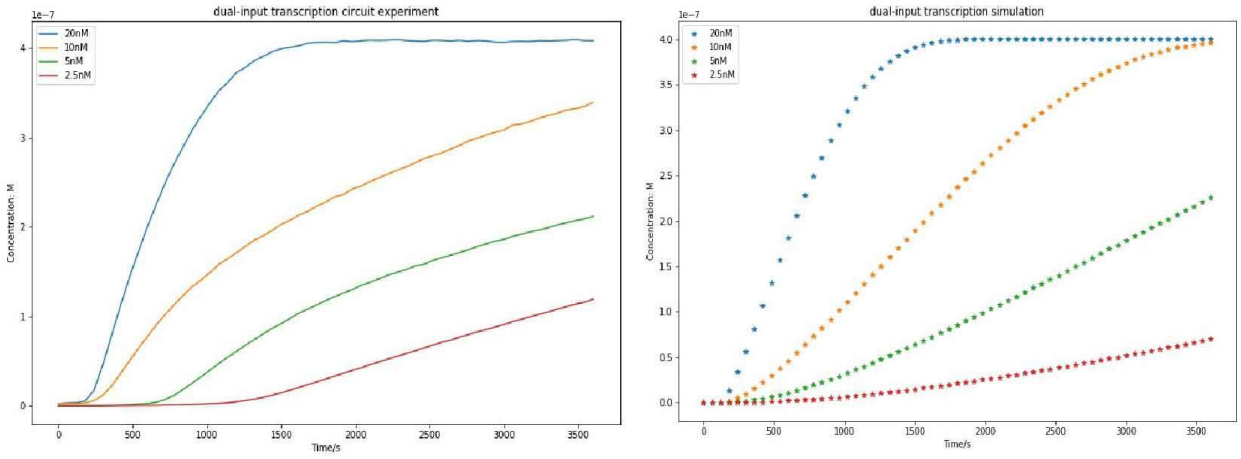

Figure S19. Kinetic characterization of the dual-input transcription circuit. (The fluorescent intensities were transformed into concentrations). Curves denote the experimental results and dots denote the simulative results. The control experiments of varying concentrations of T/B and I3 and I4: 2.5nM, 5nM, 10nM and 20nM were performed. [F/Q] =400nM.